Performance of NLOS Base Station Exclusion in cmWave 5G Positioning

Alda Xhafa*, José A. del Peral-Rosado*†, Gonzalo Seco-Granados*, José A. López-Salcedo*

* IEEC-CERES, Universitat Autònoma de Barcelona (UAB), Bellaterra, Barcelona, Spain
*† Airbus Defence and Space, Taufkirchen, Germany
Email: {alda.xhafa, joseantonio.delperal, gonzalo.seco, jose.salcedo}@uab.cat

***Abstract*—Positioning methods relying on cellular signals are subject to severe degradation errors due to the inherent harsh working conditions of urban scenarios. In contrast, emerging applications are gradually requesting a more accurate and reliable positioning solution, thus requiring the implementation of alternative measures to minimize such degradation. This paper describes a method for detecting faulty measurements from base station (BS) affected by non-line-of-sight (NLOS) propagation. The method monitors the residuals resulting from the least-squares positioning solution, inspired by the approach implemented by Receiver Autonomous Integrity Monitoring (RAIM) techniques in Global Navigation Satellite Systems (GNSS) receivers. The method has been tested through simulations based on a deep urban deployment map, which comes with an experimental data file of user's position. Positioning Reference Signal (PRS) of 5G New Radio (NR) operating in the centimeter-wave (cmWave) band is used. Results confirm the utility of implementing NLOS monitoring method to achieve a better performance assessment under realistic assumptions while using 5G positioning signals.**

***Index Terms*—Positioning, 5G cellular networks, New Radio (NR), NLOS, integrity, test statistic, cmWave.**

I. Introduction

The use of cellular networks for positioning purposes has received an increasing interest in recent years [1]. Initially, it was primarily motivated by the need to fulfill legal mandates on the user's localization accuracy, such as the Federal Communications Commission (FCC) E911 mandate and the European E112 recommendation. At that time, though, the achievable positioning performance was severely limited by network and signal design considerations, which primarily focused on voice and data communications. The trend started to change with the advent of 4G Long Term Evolution (LTE) cellular networks, where specific signals were introduced for the first time for positioning purposes, i.e., the so-called Positioning Reference Signals (PRS). Positioning is now expected to play a prominent role promoted by the emerging 5G cellular networks. Such networks will significantly increase the positioning performance through the provision of cm-accurate measurements based on millimeter-wave (mmWave) signals [2], [3].

Determining the positioning performance that can be achieved with 5G New Radio (NR) signals is of great interest to both carrier operators and network users because it enables to assess the feasibility of location-based services (LBS) and applications relying on positioning information. Unfortunately, positioning accuracy is hindered by many propagation effects such as multipath and non-line-of-sight (NLOS), which may appear due to surrounding obstacles, particularly in urban environments. These circumstances could cause poor accuracy and reliability of the computed position, and they should be therefore monitored in order to preserve the overall positioning performance. Contributions on positioning with cellular signals tend to ignore the presence of such propagation obstacles and consider instead the so-called *achievable* positioning performance [4]. Some other contributions incorporate the presence of multipath and NLOS, but no mechanisms are implemented to distinguish between LOS/NLOS situations [5].

The main objective of this work is to implement a NLOS detection mechanism for positioning with cellular signals based on a similar principle to that of Receiver Autonomous Integrity Monitoring (RAIM), a technique widely adopted in the context of Global Navigation Satellite Systems (GNSS) receivers [6]. By doing so, we are able to preserve the integrity of the position solution by detecting and removing abnormal measurements. As a by-product, we can also provide a better assessment of the actual cellular positioning performance rather than assuming ideal propagation conditions or mixing both LOS and NLOS observations as customary in many existing contributions. Furthermore, we study the limitations of the residuals-based RAIM-like implementation in cmWave 5G positioning.

The fundamental concept behind the proposed technique is to check the redundancy of range measurements obtained from all available base stations (BSs), in order to detect one faulty transmitter at a time [7]. To do so, the technique includes both a fault detection (FD) [8] and a fault-detection-and-exclusion (FDE) functionality. When there are more BS than the number of unknowns, the position solution is computed using the ranges from the minimal number of BS needed, while the ranges from the remaining BS are checked to be consistent with the computed position. If the range from a BS differs significantly from the expected value, a faulty bias is incurred by it. Then, when there is a sufficient number of BSs, the algorithm can detect which BS is causing such degradation and thus it can be removed. Each positioning solution should

This work has been partially supported by the ICREA Academia Program and the Spanish Ministry of Economy and Competitiveness projects TEC2017-89925-R and TEC2017-90808-REDT.

set a 2-D or 3-D range "tolerance limit", below which a faulty bias in the measurements is not checked.

The paper is organized as follows. Sect. II introduces the signal model, its properties as well as the position computation process. Sect. III presents the main integrity monitoring approaches [15] and analyses the limitations of the proposed method. Sect. IV describes in details the scenario used in this work and analyses the results. Finally, Sect. V draws the conclusions.

II. Signal model

A. Observables calculation

Observed Time Difference of Arrival (OTDoA) is adopted in 5G for the down-link synchronization of PRS signals [9], similar to what was already done in previous releases for 4G/LTE down-link positioning. To calculate a user's position, the distance between the user's receiver and multiple BSs with known locations must be measured. While the position computation is done by the network, the User Equipment (UE) is in charge of measuring the time delays on the synchronization signals it receives from neighboring BSs, which actually provide the euclidean distance between UE and BS. In practice, however, these measurements are affected by an unknown clock offset and noise thus leading to a so-called pseudo-distance or pseudo-range.

Let us denote by $\delta t_{5\mathrm{G}}$ the clock offset of UE with respect to reference 5G time, the j-th BS synchronization error by $e_{\mathrm{sync},j}$ and the Time Delay Estimation (TDE) error in meters by $e_{\mathrm{TDE},j}$. Then let $\mathbf{u} \doteq [x_u, y_u, z_u]^T$ be the unknown UE position and $\mathbf{b}_j \doteq [x_{b,j}, y_{b,j}, z_{b,j}]^T$ the known j-th BS position among N available BSs, which are closer in distance with UE, relative to a reference coordinate. The ranging errors, which are added to the euclidean BS-UE distance, are calculated here by taking into account the LOS conditions, the Signal-to-noise ratio (SNR) levels and a random probability variable drawn from a uniform distribution between 0 and 1 following the physical-layer abstraction of 5G observables proposed in [10]. As a result, the pseudo-range from the UE to the j-th BS is expressed with the formula $\rho_j \doteq \| \mathbf{b}_j - \mathbf{u} \| + c\delta t_{5\mathrm{G}} + e_{\mathrm{sync},j} + e_{\mathrm{TDE},j}$.

Calculating the differences of Time of Arrival (ToA) observables eliminates δt_{5G} and yields the OTDoA measurement in the time domain. In this work, it is also assumed a perfectly synchronized network among BSs, so $e_{\mathrm{sync},j}$ is not considered. Thus, the jth OTDoA observable is calculated as the time difference of pseudo-ranges from the serving and neighbour BSs. We consider the first BS (the most powerful, with the highest SNR), as the reference so that $\rho_{\mathrm{OTDoA},j} \doteq \rho_1 - \rho_{j+1}$ for $j = 1, \ldots, N-1$ where ρ_1 is the pseudo-range observable from the serving BS and ρ_{j+1} the pseudo-range observable from the $(j+1)$-th neighbour BS with N the total number of BSs used for positioning. Hence, the SNR levels are considered for sorting the ascending list of BSs.

B. Position computation

It is worth noting that ρ_j is a non-linear function of the user's position. However, it can be linearised using its Taylor series around a tentative user's position $\hat{\mathbf{u}} \doteq [\hat{x}_u, \hat{y}_u, \hat{z}_u]^T$. Using the tentative position, we calculate the approximate pseudo-range: $\hat{\rho}_j \doteq \| \mathbf{b}_1 - \hat{\mathbf{u}} \| - \| \mathbf{b}_{j+1} - \hat{\mathbf{u}} \|$, for $1 \leq j < N-1$. Having $N \geq 4$ BSs in order to provide a single solution, the solution of the unknown 3D receiver position $\mathbf{u}$ is solved based on the conventional least squares (LS) solution of the OTDoA positioning problem by using the well-known iterative Gauss-Newton (GN) method. The GN solution at the l-th iteration is $\hat{\mathbf{u}}_l = \hat{\mathbf{u}}_{l-1} + (\mathbf{H}^T\mathbf{H})^{-1}\mathbf{H}^T(\hat{\boldsymbol{\rho}}(\hat{\mathbf{u}}_{l-1}) - \boldsymbol{\rho}_{\mathrm{OTDoA}})$, where $\hat{\boldsymbol{\rho}}(\hat{\mathbf{u}}_{l-1}) \doteq [\hat{\rho}_1(\hat{\mathbf{u}}_{l-1}), \ldots, \hat{\rho}_{N-1}(\hat{\mathbf{u}}_{l-1})]^T$ is the vector of measured pseudo-ranges corresponding to the linearization reference position, $\boldsymbol{\rho}_{\mathrm{OTDoA}} = [\rho_{\mathrm{OTDoA},1}, \ldots, \rho_{\mathrm{OTDoA},N-1}]^T$ is the vector of predicted pseudo-ranges corresponding to the real receiver position and $\mathbf{H}$ is the geometry matrix defined as $[\mathbf{H}]_{j,1:3} \doteq \left[\frac{\mathbf{b}_1 - \hat{\mathbf{u}}}{\|\mathbf{b}_1 - \hat{\mathbf{u}}\|} - \frac{\mathbf{b}_{j+1} - \hat{\mathbf{u}}}{\|\mathbf{b}_{j+1} - \hat{\mathbf{u}}\|} \right]$. We ensure full rank of $\mathbf{H}$, which guarantees the invertibility of $\mathbf{H}^T\mathbf{H}$.

The GN method often converges quickly, especially when the iteration begins with a reference position close enough to the true position. However, if the iteration begins far from the target position, convergence may be slow or not achieved at all. To avoid this problem, a tolerance level is set to ensure that the range residual parameters (i.e. the difference between the predicted range and pseudo-range measurements) do not exceed the level set by the user. The tolerance level has been set based on Monte Carlo simulation results.

III. NLOS BS exclusion mechanism

The process for monitoring the measurements and eventually excluding faulty BS is done following the flow diagram depicted in Fig. 1.

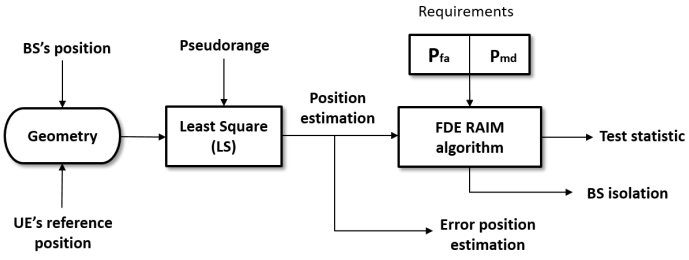

Fig. 1. NLOS BS exclusion mechanism.

The proposed method processes the incoming measurements and solves the UE position. Before the NLOS exclusion starts, it is assumed that the UE position was already estimated by the LS as stated in Sect. II-B, so that a reasonable starting position could be used to ensure the convergence of the GN method. The following steps are then implemented:

1) Calculate the pseudo-range residuals using all BSs in the scenario. Large residuals indicate that a measurement error (bias) might be present. Generally, to perform a fault detection there must be at least one redundant observation available. Since we are working with OTDoA, a minimum

of four BSs are needed to compute a 3D position, five BSs to detect a failure and six BS to detect and exclude the faulty BS.

2) If a failure is detected, we create subsets of BSs by setting one BS as serving for the OTDoA measurements and removing one BS from the rest of BSs at a time, so there will be $(N-1)$ subsets, each having $(N-1)$ BSs. The user's position obtained from any of these subsets might indicate the presence of an inconsistent measurement if it exhibits an offset larger than the range set in the "tolerance limit". The detection of the failure is achieved by performing a consistency check through a test statistic parameter.
3) The test statistic is related to pseudo-range observations and compared to a threshold in order to detect a faulty BS. We set the probability of missed detection for the level of acceptance of the parameter of control by determining the minimum detectable bias. Note that it is not always possible to identify a faulty BS.

A. Computation of test statistic

The network provides a LS estimate of the position based on OTDoA measurements. This is done using the linearised measurement equation: $\Delta\boldsymbol{\rho} = \mathbf{H}\mathbf{u}$, where $\Delta\boldsymbol{\rho}$ is the range residual vector containing the difference of measured and predicted pseudo-range (the latter coming from the previous estimate of user's position in Sect. II-B), $\mathbf{H}$ is the geometry matrix as stated in Sect. II-B, and $\mathbf{u} \doteq [x_u, y_u, z_u]^T$ is the vector containing the coordinates of the user's position.

Therefore, the LS estimate of $\mathbf{u}$ is $\hat{\mathbf{u}} = (\mathbf{H}^T\mathbf{H})^{-1}\mathbf{H}^T\Delta\boldsymbol{\rho}$. The geometry matrix is decomposed into the signal matrix ($\mathbf{U}_S$) and noise matrix ($\mathbf{U}_N$) through QR factorization [11]. The dimension of the noise subspace is $(N-4)$. In the absence of any fault, the noise subspace should only contain the noisy contribution of the LS residuals and thus it could be modeled as a subspace of zero-mean Gaussian random vectors [12]. However, when a bias is present, the noise subspace will be distorted by the faulty bias and the noise-only condition will be not cut-clear. The QR factorization is preferable instead of performing conventional orthogonal matrix projection because it requires less computations and allows to easily distinguish the noise from the signal by visualizing the presence of any degradation. These constitutes the building blocks for the detection method to be described in III-B.

The LS residuals on which the detection is implemented are obtained as follows: $\mathbf{v} = \Delta\boldsymbol{\rho} - \mathbf{H}\,\hat{\mathbf{x}} = \mathbf{U}_N^T\,\Delta\boldsymbol{\rho}$, where $\mathbf{U}_N^T$ is a $(N-4)\times(N-1)$ matrix whose rows are mutually orthogonal. In order to detect a faulty BS, the test statistic of each subset is formed from the Sum of Squared Residuals (SSR), $\mathrm{SSR_i} \doteq \mathbf{v}_\mathrm{i}^T\mathbf{M}_\mathrm{i}\mathbf{v}_\mathrm{i}$, where $\mathbf{M}_\mathrm{i}$ is the matrix of eigenvectors of noise that does the normalization of range residuals through the whitening process. The test statistic should follow a normalized χ^2 distribution with $N-4$ degrees of freedom (DOF). If any measurement error is biased, the distribution will then be non-central χ^2 with the same degree of freedom.

The i-th test statistic for $i = 1, 2, ..., N-1$ subsets formulated from the SSR is given by $T_i \doteq \sqrt{\mathrm{SSR_i}/(N-4)}$ and its value depends on both the pseudo-range measurements and the geometry of the user and base station. The decision variable T_i is tested against a threshold γ (see next subsession). Thus, the detection is based on a hypothesis testing where a measurement is considered faulty when $T_i > \gamma$.

B. The selection of threshold parameter

The selection of the threshold is done analytically based on the requirements for false alarm [11]. For a cumulative distribution function (CDF) of test statistic values, the quantile α defines the probability of detecting bias-free BSs subsets. Denoting the threshold γ as that providing a specific probability of false alarm ($\mathrm{P_{fa}}$), the following relationship holds: $\mathrm{P_{fa}}(\gamma) = 1 - \alpha(\gamma) = 1 - \int_0^\gamma f_{\chi^2}(T)dT$. The sum of squared residuals T_i follows a centralized χ^2 distribution with $N-4$ DOF. This means that, for instance in case of having seven BSs, four BSs are needed to determine position $\mathbf{u}$ and the rest contribute to the error. The pseudo-range measurements should be uncorrelated and have a unit variance to follow a desirable normalized χ^2 distribution.

IV. Simulation Results and Evaluation

A. Scenario definition

In this work, a predefined urban macro-cell (UMa) network scenario based on a deep urban deployment map is considered with seven BSs surrounded by high buildings and UE located outdoors at street level. NLOS propagation is common in urban environments, as considered in [10], [14]. Simulations are done for the use case of high-accuracy autonomous cars. The coordinates used are in ENU (East, North, Up) relative to a near reference location.

As explained in Sect. III, the minimum number of BSs to perform detection and exclusion of the faulty BS is six, the reason being that we are using OTDoA, which gives one measurement less than the conventional ToA usually used in RAIM. The FDE is performed at any subset of $(N-1)$ BSs. The subsets are created by keeping the first BS as reference for OTDoA measurements and by removing one BS at a time from the rest of serving BSs. Since the accuracy of the estimated position depends upon the BS and UE geometry [13], we ensure that the geometry of our scenario has a horizontal dilution of precision (HDOP) smaller than 2. As we are dealing with a terrestrial deployment with BSs at similar heights, vertical accuracy tend to be rather poor, however we are only interested in the horizontal positioning.

The simulation is done based on the UMa channel model defined in [14]. The distance between BS and UE is used to determine the propagation conditions based on distance-dependent LOS probability and path loss models tabulated in [14]. These conditions are compared in terms of LOS/NLOS conditions and SNR levels (limited between -30dB and 30dB) for an UMa environment. The ranging observables are calculated for specific propagation conditions, channel model, system bandwidth (BW), SNR levels and time-delay estimator.

A 5G PRS signal with a BW of 20 MHz and 100 MHz at a carrier frequency of 2 GHz, within the cmWave Frequency

Range 1 (FR1) of 5G NR has been considered. For simplicity, the network is supposed to be perfectly synchronized among BSs. The Time Delay Estimator (TDE) error is obtained as the time-delay measurement of the first correlation peak above a threshold through the threshold-based estimator presented in [10].

B. Implementation and performance results

The UE is initially in "cold start" and has no previous information about its position. Firstly, the position is estimated assuming ideal conditions (no multi-path and LOS scenario) and trilaterating the distances between all BS. Then the LS positioning method is run with 300 Monte Carlo iterations for each UE position.

To check the capability of the method to identify the anomalous measurements, a bias ranging from 5 to 100 meters is added to the ranging error of the second BS of our scenario in the Monte Carlo simulations. The probability of false alarm is set to $P_{\text{fa}} = 0.2$, resulting in a threshold of $\gamma = 1$ m calculated as explained in Sect. III-B. The presence of a fault measurement (faulty bias) is distinguished between bias-free measurements through the test statistic, a parameter that gives information about pseudo-range measurement errors. After the ith test statistic T_i is computed for each subset of BSs, it is compared against the given threshold. If the test statistic exceeds the given threshold value, a bias might be present. In the subset where the tests statistic are smaller than the given threshold, the missing BS is assumed to be faulty and hence excluded. Thus, the estimate of the user's position is performed without this BS. In the figures presented herein, the CDFs of T_i of each subset are given, where the part of the curve with the colored area underneath gives the T_i that are smaller than the given threshold.

1) Results when BW=20 MHz: Fig. 2 and Fig. 3 present the CDFs of each T_i, where a bias of 5 m and 30 m respectively is added to the measurements. We have shown these two cases because the first one represents the lower limit of the bias considered in this work, and the second one represents a bias for which a significant improvement of the positioning accuracy starts to be noticed. According to the results, with a 30 m bias, the subset with the second BS missing shows that 81% of the test statistic calculated for each Monte Carlo iteration is smaller than the given threshold. This is a significantly high percentage compared to the other subsets, where the test statistic exceeds the given threshold. The achieved results allow us to deduce that the second BS is the faulty one. However, since the differential pseudo-range measurements are slowly varying, is not always easy to apply a fixed threshold to the test statistic. This is noticed with small biases, when the resulting error is more difficult to be detected. For instance, in the case of 5 m bias depicted in Fig. 3 the presence of the bias becomes less easy to be detected than before. In each subset there is a percentage where the calculated test statistic is smaller than the given threshold. Also, the use of a small bandwidth affects the accuracy of OTDoA measurements and the ability of LS algorithm itself

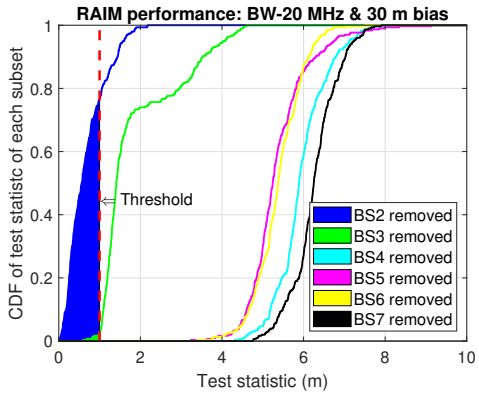

Fig. 2. CDF of the NLOS test T for BW=20 MHz with an 30 m bias.

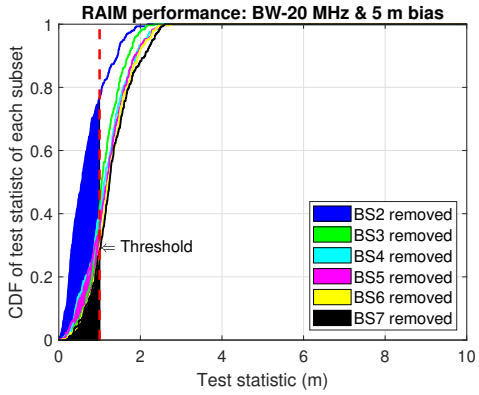

Fig. 3. CDF of the NLOS test T for BW=20 MHz with an 5 m bias.

to dissolve or minimize the error, and therefore can affect the performance of RAIM.

2) Results when BW=100 MHz: Results in Fig. 4 show that the second BS is the faulty one, because removing it makes that 80% of the calculated tests statistic are smaller than the given threshold, while its presence makes that all tests statistic exceed the given threshold. Despite having similar results with the previous scenario, the use of a bigger bandwidth makes the detection of bias easier for the case in Fig. 5 and therefore the monitoring integrity method is more reliable.

Apart from observing the statistical performance of the proposed NLOS test, it is important to assess the actual gain we obtain in terms of the UE positioning performance. Fig. 6 and Fig. 7 present the UE horizontal position errors for the cases when the NLOS detection method is used and when it is not. In conditions of perfect network synchronization, with the use of wide bandwidth, we expect optimistic results that meet the performance target, where the OTDoA horizontal positioning error is smaller than 10 m for 80% of UEs in outdoor deployments scenarios. However, a significant degradation of the OTDoA accuracy is noticed when the NLOS exclusion method is not used, even for the case of maximum bandwidth. In both figures (Fig. 6 and Fig. 7), it can be seen that the probability of having a position error smaller than 10 m is significantly higher when the method is used. On the

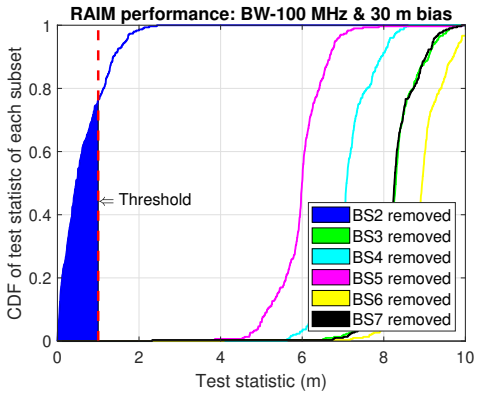

Fig. 4. CDF of the NLOS test T of BW=100 MHz with an 30 m bias.

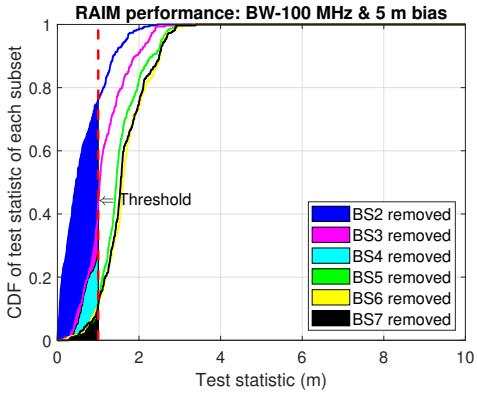

Fig. 5. CDF of the NLOS test T for BW=100 MHz with an 5 m bias.

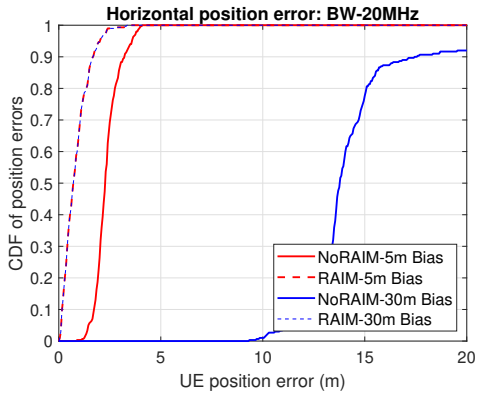

Fig. 6. UE error positions when using RAIM or not.

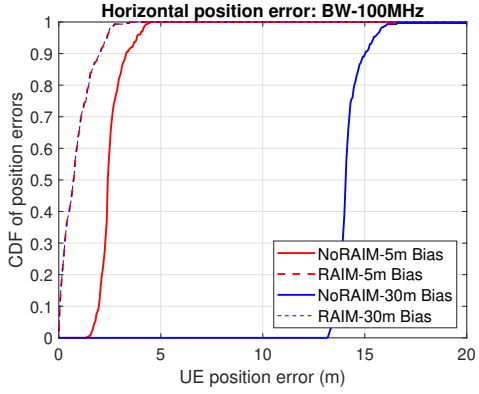

Fig. 7. UE error positions when using RAIM or not.

other hand, for the case of small bias, is not always possible to detect the faulty BS. We believe this happens because it is more difficult to discern the wrong measurement when the error is more precise.

General observations on the simulation results have shown that the proposed method is able to detect a bias as low as 2 m and hence exclude the faulty BS. Moreover, the maximum horizontal position error is reduced by 55.6% on average.

V. Conclusions

This paper has shown the advantages provided by the exclusion of BS affected by NLOS, which is a frequent situation in 5G positioning when operated in urban environments. A RAIM-like algorithm has been proposed based on the analysis of the LS residuals when obtaining the positioning solution. Results from simulations of an urban channel model with seven visible BSs confirm the usefulness of the proposed approach and thus the benefits of incorporating such mechanisms in the assessment of the realistic 5G positioning performance.

References

[1] J. A. del Peral-Rosado, R. Raulefs, J. A. López-Salcedo, and G. Seco-Granados, "Survey of cellular mobile radio localization methods: From 1G to 5G," *IEEE Com. Surveys & Tutorials*, 20(2):1124–1148, 2018.

[2] A. Dammann, R. Raulefs, and S. Zhang, "On prospects of positioning in 5G," in *Proc. IEEE ICCW*, 2015, pp. 1207–1213.

[3] H. Wymeersch, G. Seco-Granados, G. Destino, D. Dardari, and F. Tufvesson,"5G mmwave positioning for vehicular networks," *IEEE Wireless Communications*, 24(6):80–86, 2017.

[4] J. A. del Peral-Rosado, J. A. López-Salcedo, G. Seco-Granados, F. Zanier, and M. Crisci, "Achievable localization accuracy of the positioning reference signal of 3GPP LTE," in *ICL-GNSS*, 2012, pp.1–6.

[5] K. Shamaei and Z. M. Kassas, "LTE receiver design and multipath analysis for navigation in urban environments," *Navigation*, 65(4):655–675, 2018.

[6] R. Grover Brown, "A baseline GPS RAIM scheme and a note on the equivalence of three RAIM methods," *Navigation*, 39(3):301–316, 1992.

[7] B. W. Parkinson and P. Axelrad, "Autonomous GPS integrity monitoring using the pseudorange residual," *Navigation*, 35(2): 255–274, 1988.

[8] M. Sturza, "Fault detection and isolation (FDI) techniques for guidance and control systems," *NATO AGARD Graph GCP/AG.314, Analysis, Design and Synthesis Methods for Guidance and Control Systems*, 1988.

[9] 3GPP, "Stage 2 functional specification of user equipment (UE) positioning in NG-RAN," Tech. Rep. TS 38.305, v15.5.0, Dec. 2019.

[10] J. A. del Peral-Rosado, F. Gunnarsson, S. Dwivedi, S. Modarres Razavi, O. Renaudin, J. A.López-Salcedo and G. Seco-Granados, "Exploitation of 3D City Maps for Hybrid 5G RTT and GNSS Positioning Simulations", *ICASSP*,pp. 9205-9209, 2020.

[11] R. Grover Brown and G. Y. Chin, "Calculation of thresholds and protection radius using chi square methods-a geometric approach," *Navigation*, vol. V, pp. 155–179, 1997.

[12] J. De Heus, "Data-snooping in control networks," in *Proc. of Survey Control Networks, Meeting of the Study Group 5B*, 1982, pp. 211–224.

[13] A. Brown and M. Sturza, "The effect of geometry on integrity monitoring performance," in *Proc. of the Inst. of Nav. Annual Meeting*, 1990.

[14] 3GPP, "Study on channel model for frequencies from 0.5 to 100 GHz," Tech. Rep. TS 38.901, Re.14, Dec. 2017.

[15] 3GPP, "TP for Study on Positioning Integrity and Reliability," R2-2006541, Re.17, Aug. 2020.